IJE TRANSACTIONS A: Basics Vol. 33, No. 4, (April 2020) 586-597

International Journal of Engineering

Journal Homepage: www.ije.ir

Space Vector Pulse Width Modulation with Reduced Common Mode Voltage and Current Losses for Six-Phase Induction Motor Drive with Three-Level Inverter

M. J. Zandzadeh[a], M. Saniei*[a], R. Kianinezhad[b]

[a] *Department of Electrical Engineering, Faculty of Engineering, Shahid Chamran University of Ahvaz, Ahvaz, Iran*
[b] *Barkhat Institute of Higher Education, Ahvaz, Iran*

PAPER INFO

Paper history:
Received 13 January 2020
Received in revised form 13 February 2020
Accepted 04 March 2020

Keywords:
Space Vector Pulse Width Modulation
Common Mode Voltage
Current Losses
Six-Phase Induction Motor
Three-Level Inverter

ABSTRACT

Common-mode voltage (CMV) generated by the inverter causes motor bearing failures in multiphase drives. On the other hand, presence of undesired z-component currents in six-phase induction machine (SPIM) leads to extra current losses and have to be considered in pulse width modulation (PWM) techniques. In this paper, it is shown that the presence of z-component currents and CMV in six phase drive system are two major limiting factors in space vector selection. The calculated voltage space vectors for both symmetrical and asymmetrical SPIM drive system with three-level inverter are illustrated in the decoupled subspaces and described in terms of undesirable voltage components and CMV value. Several space vector pulse width modulation (SVPWM) techniques are investigated based on CMV and z-component currents generation. Then, a modified SVPWM technique with minimum current distortion, undesired current components and CMV with a modest torque ripple is proposed based on the simulation results.

***doi**: 10.5829/ije.2020.33.04a.10*

NOMENCLATURE

V_s , V_r	Stator and rotor voltage vectors	S_i	Statte of i^th phase leg
R_s , R_r	Stator and rotor resistance matrices	T_s	Sampling time interval
I_s , I_r	Stator and rotor current vectors	f_s	Fundamental frequency
L_s , L_r	Stator and rotor inductance matrices	**Greek Symbols**	
L_{ls} , L_{lr}	Stator and rotor leakage inductances	ω_r	Rotor angular speed
T_e	Electromagnetic Torque	γ	Phase difference between two three phase windings
P	Induction machine Pole number	**Subscripts**	
p	Derivative operator	a, b, c, d, e, f	Stator phasee name
V_{dc}	DC link voltage	α and β	Alpha and beta axis
V_{cm}	Common mode voltage	z_1, z_2, z_3 and z_4	z-compnents axis

1. INTRODUCTION

Multiphase induction motor drives have been widely explored in recent years because of their advantages compared with traditional three phase systems such as higher torque density, lower torque pulsation and fault tolerance ability [1]. They are being considered as a proper alternative in marine electric propulsion [2], electric or hybrid vehicles, and high power applications [3].

The six-phase induction machine (SPIM) is one of the most popular configurations, and is divided in two types

*Corresponding Author Email: *m.saniei@scu.ac.ir* (M. Saniei)

Please cite this article as: M. J. Zandzadeh, M. Saniei, R. Kianinezhad, Space Vector Pulse Width Modulation with Reduced Common Mode Voltage and Current Losses for Six-Phase Induction Motor Drive with Three-Level Inverter, International Journal of Engineering (IJE), IJE TRANSACTIONS A: Basics Vol. 33, No. 4, (April 2020) 586-597

of symmetrical and asymmetrical with 60 and 30 electrical degrees spatially phase shifted between two sets of three-phase windings.

Presence of z-component currents in SPIM due to PWM voltage generated by the inverter produces harmonic currents that do not contribute to the air gap flux and torque production, circulate in phase stator windings, and generate additional losses. This can reduce the system efficiency and increase size and cost of the machine drive system [4].

Many researches have been done to reduce harmonic currents by applying proper PWM techniques. In these PWM methods, the voltage space vectors are selected based on minimum undesirable z-component voltage production and as a result, a few number of vectors can be selected despite the large number of space vectors in compared with three phase drives [5-9].

Common-mode voltage (CMV) is one of the problems associated with variable speed drive. The high frequency, high amplitude and large step size (dv/dt) of CMV produces bearing currents via parasitic capacitances which may lead to insulation and bearing failures [10], mechanical vibration [11] and also bearing undesirable electromagnetic interference (EMI) [12]. Several PWM techniques based on sinusoidal PWM [13-15] or SVPWM [16-20] strategies have been applied to reduce the CMV in multiphase systems. The researchers tried to reduce the CMV by phase shifting of carrier signal in control system of five-phase and six-phase (both symmetrical and asymmetrical) two-level voltage source inverters feeding R-L load, which leads to higher phase current harmonic and distortion [13]. In literature, [14-15] three career based PWM methods were analyzed in terms of CMV generation on a five phase coupled-inductor inverter with R-L load. Chen and Hsieh [16] proposed a pulse-width modulator with minimum CMV for generalized two-level N-phase voltage source inverters with odd phase numbers, and used vectors with minimum CMV. A multidimensional strategy was proposed in literature [17] to eliminate the CMV in generalized multiphase multilevel inverter by selecting switch states with zero CMV. But this method is suitable only for multilevel inverters with a level number higher than three. Two PWM techniques were proposed in literature [18, 19] for the linear and over-modulation regions that result in 40 and 80% CMV peak-to-peak reduction in five-phase inverter respectively. Dabour et al. [20] mitigated the CMV by classifying the space vectors based on their corresponding CMV level in a three to five-phase matrix converter and reduced the peak amplitude of CMV to 48%.

Although intensive researches have been done on modifying PWM methods to reduce the CMV, not enough work has been done on PWM methods with CMV reduction for six-phase drives. Moreover**,** most of the mentioned researches for reducing the CMV were done on multiphase inverter with an R-L, and the machine performance like electromagnetic torque ripple is not analyzed. Also, the presence of undesirable z-component currents in SPIM imposes a considerable limitation in PWM method (because lower number of space vectors can be applied) and it may lead to a challenge with CMV eliminating or reducing techniques, and is not considered in the above mentioned studies [13-16] and [20]. On the other hand, many researchers tried to reduce z-component currents in multi-phase drives without considering CMV production [5-9].

In our previous research [21], it is shown that z-component mitigation and CMV elimination problems cannot be achieved simultaneously in a single neutral SPIM drive system with two-level inverter despite having larger space vectors number than three-phase drive. Hence, it is tried to overcome the limitations in this paper by exploring space vectors in a three-level inverter. For this purpose, the calculated voltage space vectors in three-level inverter are categorized in decoupled subspaces and described in terms of undesirable voltage components and CMV value. The selected space vectors (based on the above limitations) is applied in several SVPWM strategies and a comprehensive comparison is performed including current distortion, CMV production and electromagnetic torque ripple. The SVPWM strategies analysis is performed on both symmetrical and asymmetrical SPIM configurations, and finally the best SVPWM strategy is proposed for both SPIM configurations based on theoretical analysis and simulation results. The CMV generated by the inverter has a considerable amplitude and high frequency waveform. Hence, removing it by the proposed method in higher frequency applications may be more useful but inverter switches with higher switching frequency must be applied.

2. MODEL OF SPIM

The circuit diagram of SPIM is shown in Figure 1. The voltage equations of stator and rotor are as follow:

$$\begin{cases} [V_s]=[R_s][I_s]+\dfrac{d}{dt}([L_{ss}][I_s]+[L_{sr}][I_r]) \\ [V_r]=[R_r][I_r]+\dfrac{d}{dt}([L_{rr}][I_r]+[L_{rs}][I_s]) \end{cases} \tag{1}$$

where the voltage and current vectors are:

$$\begin{aligned} &[V_s]=[0\quad 0\quad 0\quad 0\quad 0\quad 0]^T \\ &[V_r]=[0\quad 0\quad 0\quad 0\quad 0\quad 0]^T \\ &[I_s]=[i_{sa}\quad i_{sb}\quad i_{sc}\quad i_{sd}\quad i_{se}\quad i_{sf}]^T \\ &[I_r]=[i_{ra}\quad i_{rb}\quad i_{rc}\quad i_{rd}\quad i_{re}\quad i_{rf}]^T \end{aligned} \tag{2}$$

As shown in [22], the SPIM model can be decomposed into three two-dimensional orthogonal subspaces, (α,β), (z_1,z_2) and (z_3,z_4), by transformation (3), where γ can be 60^0 or 30^0 electrical degrees for symmetrical and asymmetrical SPIM respectively.

$$[T]=\frac{1}{\sqrt{3}}\begin{bmatrix} 1 & \cos(\gamma) & -1/2 & \cos(2\pi/3+\gamma) & -1/2 & \cos(4\pi/3+\gamma) \\ 0 & \sin(\gamma) & \sqrt{3}/2 & \sin(2\pi/3+\gamma) & -\sqrt{3}/2 & \sin(4\pi/3+\gamma) \\ 1 & \cos(\pi-\gamma) & -1/2 & \cos(\pi/3-\gamma) & -1/2 & \cos(5\pi/3-\gamma) \\ 0 & \sin(\pi-\gamma) & -\sqrt{3}/2 & \sin(\pi/3-\gamma) & \sqrt{3}/2 & \sin(5\pi/3-\gamma) \\ 1 & 0 & 1 & 0 & 1 & 0 \\ 0 & 1 & 0 & 1 & 0 & 1 \end{bmatrix} \quad (3)$$

By applying Equation (3) into the voltage Equation (1), a new decoupled system is obtained for SPIM. The stator and rotor voltage equations for (α,β), (z_1,z_2) and (z_3,z_4) subspaces are achieved as below:

$$\begin{bmatrix} v_{s\alpha} \\ v_{s\beta} \\ 0 \\ 0 \end{bmatrix}=\begin{bmatrix} r_s+L_s p & 0 & Mp & 0 \\ 0 & r_s+L_s p & 0 & Mp \\ Mp & \omega_r M & r_r+L_r p & \omega_r L_r \\ -\omega_r M & Mp & -\omega_r M & r_r+L_r p \end{bmatrix}\begin{bmatrix} i_{s\alpha} \\ i_{s\beta} \\ i_{r\alpha} \\ i_{r\beta} \end{bmatrix} \quad (4)$$

$$\begin{bmatrix} v_{sz1} \\ v_{sz2} \end{bmatrix}=\begin{bmatrix} r_s+L_{ls} p & 0 \\ 0 & r_s+L_{ls} p \end{bmatrix}\begin{bmatrix} i_{sz1} \\ i_{sz2} \end{bmatrix} \quad (5)$$

$$\begin{bmatrix} 0 \\ 0 \end{bmatrix}=\begin{bmatrix} r_r+L_{lr} p & 0 \\ 0 & r_s+L_{lr} p \end{bmatrix}\begin{bmatrix} i_{rz1} \\ i_{rz2} \end{bmatrix} \quad (6)$$

$$\begin{bmatrix} v_{sz3} \\ v_{sz4} \end{bmatrix}=\begin{bmatrix} r_s+L_{ls} p & 0 \\ 0 & r_s+L_{ls} p \end{bmatrix}\begin{bmatrix} i_{sz3} \\ i_{sz4} \end{bmatrix} \quad (7)$$

$$\begin{bmatrix} 0 \\ 0 \end{bmatrix}=\begin{bmatrix} r_r+L_{lr} p & 0 \\ 0 & r_s+L_{lr} p \end{bmatrix}\begin{bmatrix} i_{rz3} \\ i_{rz4} \end{bmatrix} \quad (8)$$

in which $M=3L_{ms}$, $L_s=L_{ls}+M$ and $L_r=L_{lr}+M$.

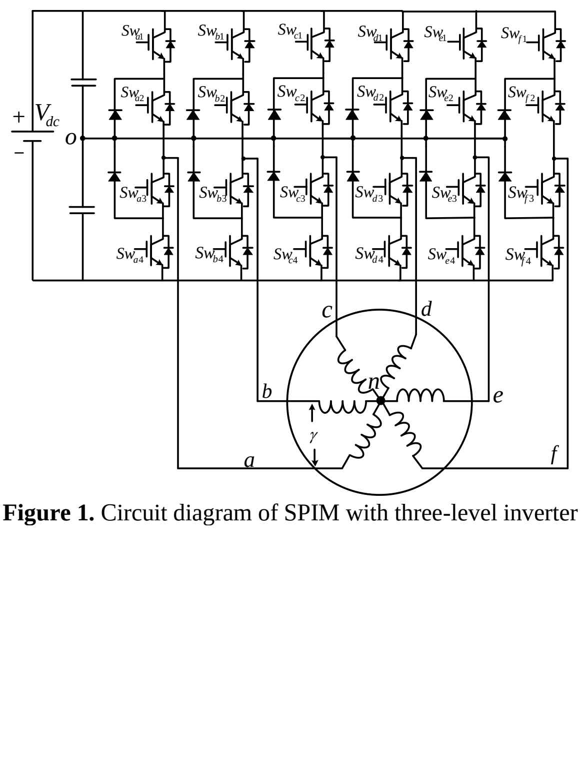

Figure 1. Circuit diagram of SPIM with three-level inverter

Based on Equations (4)-(8) the electromechanical torque of machine can be calculated as follows [9]:

$$T_e=\frac{P}{2}M(i_{s\beta}\,i_{r\alpha}-i_{s\alpha}\,i_{r\beta}) \quad (9)$$

According to Equation (9) the z_1 to z_4 current components have no effect on electromagnetic torque, and as can be seen in Equations (5)-(8) the machine model in (z_1,z_2) and (z_3,z_4) subspaces are presented as a R-L circuit with no back EMF (ElectroMotive Force) voltage term. These current components can be so high in amplitude, depending on applied PWM technique, and may lead to extra copper losses and undesired current distortion. So, the z-component currents must be considered in SPIM drive control system.

3. THREE-LEVEL 6-PHASE INVERTER

3. 1. Stator Phase Voltages Based on Figure 1, the output voltage per phase (with respect to midpoint of the DC bus) in three-level six-phase inverter can be written as a function of switching states:

$$\begin{bmatrix} v_{oa} \\ v_{ob} \\ v_{oc} \\ v_{od} \\ v_{oe} \\ v_{of} \end{bmatrix}=\frac{V_{dc}}{2}\begin{bmatrix} S_a \\ S_b \\ S_c \\ S_d \\ S_e \\ S_f \end{bmatrix} \quad (10)$$

where switching states S_a, S_b, S_c, S_d, S_e and S_f can be 0, -1 or 1 depending on the switches state shown in Table 1.

So, there are 3^6=729 switching states for a three-level six-phase inverter. According to Figure 1, The stator phase voltages (with respect to point 'n') can be calculated as below:

$$\begin{cases} v_{sa}=v_{oa}-v_{on} \\ v_{sb}=v_{ob}-v_{on} \\ v_{sc}=v_{oc}-v_{on} \\ v_{sd}=v_{od}-v_{on} \\ v_{se}=v_{oe}-v_{on} \\ v_{sf}=v_{of}-v_{on} \end{cases} \quad (11)$$

TABLE 1. S_i values $(i=a,b,c,d,e,f)$ and corresponding output voltages for different switches states

S_i	V_{oi}	S_{wi1}	S_{wi2}	S_{wi3}	S_{wi4}
1	$+\frac{V_{dc}}{2}$	on	on	off	off
0	0	off	on	on	off
-1	$-\frac{V_{dc}}{2}$	off	off	on	on

where $v_{on}= v_n - v_o$.
Assuming six phase balance of stator windings results in:

$$v_{sa}+v_{sb}+v_{sc}+v_{sd}+v_{se}+v_{sf}=0 \tag{12}$$

So, v_{on} can be calculated using Equations (11) and (12):

$$v_{on}=\frac{1}{6}(v_{ao}+v_{bo}+v_{co}+v_{do}+v_{eo}+v_{fo}) \tag{13}$$

By manipulating Equations (10), (11) and (13) the stator phase voltages can be shown by Equation (14).

$$V_s=\frac{1}{6}\frac{V_{dc}}{2}\begin{bmatrix}5 & -1 & -1 & -1 & -1 & -1\\ -1 & 5 & -1 & -1 & -1 & -1\\ -1 & -1 & 5 & -1 & -1 & -1\\ -1 & -1 & -1 & 5 & -1 & -1\\ -1 & -1 & -1 & -1 & 5 & -1\\ -1 & -1 & -1 & -1 & -1 & 5\end{bmatrix}\begin{bmatrix}S_a\\ S_b\\ S_c\\ S_d\\ S_e\\ S_f\end{bmatrix} \tag{14}$$

The voltage vector calculated by Equation (14) can be projected on the α-β, z_1-z_2 and z_3-z_4 planes using the transformation (3). By adding "1" to all characters of each switching state and converting the resulted six-bit ternary number to decimal, the number of corresponding space vector can be determaind. For example, switching state (1 0 -1 -1 0 1) is changed into ternary number of (2 1 0 0 1 2) corresponding to the space vector with number 572.

3. 2. Common Mode Voltage Calculation The common mode voltage can be considered as the voltage between the load neutral point and the midpoint of the DC bus [13]. So, the CMV is the same as v_{on} in Equation (13) and is given by:

$$v_{cm}=\frac{1}{6}\sum v_{io}=\frac{1}{6}\frac{V_{dc}}{2}\sum S_i \quad , \ i=a,b,c,d,e,f \tag{15}$$

The space vectors are categorized in Table 2 based on CMV generation. As can be seen, the 13-level of CMV is generated in a three-level inverter and there is a symmetry in the number of vectors with opposite sign of CMV. Hence, the property of the CMV waveform directly depends on the selected space vectors in the applied PWM technique.

4. SPACE VECTOR PWM

4. 1. Symmetrical SPIM Since projected model on the α-β plane is associated with the electromechanical energy conversion, it is clear that the applied PWM strategy must generate maximum voltage in the α-β plane while having zero or minimum amplitude in the z_1-z_2 and z_3-z_4 planes.

The first vector group with highest amplitude in the α-β plane (1.155 pu) is depicted in Figure 2. The selected space vectors have 0 and 0.408 pu amplitude in the z_1-z_2 and z_3-z_4 planes respectively and adjacent vectors in the α-β plane have opposite direction in the z_3-z_4 plane. The sum of switches state for all the selected space vectors is zero. So, based on Equation (15), no CMV is produced by applying them. The space vector number 364 with switching state of (0 0 0 0 0 0) can be considered as zero vector which produces no CMV and z-component voltage.

According to the above space vector selection, the α-β plane is divided into six sectors. The balanced six-phase sinusoidal reference voltages have no z-component in the orthogonal subspaces and just consists of α-β components. So, to generate the reference voltage in the orthogonal subspaces, balanced volt-second described in Equation (16) must be considered based on reference voltage position in the α-β plane. To equalize the number of equations and unknown variables and achieving unique answer for time intervals, four active vectors must be selected.

$$\begin{cases}V_{1\alpha}T_1+V_{2\alpha}T_2+V_{3\alpha}T_3+V_{4\alpha}T_4+V_{0\alpha}T_0=V_\alpha^* T_1\\ V_{1\beta}T_1+V_{2\beta}T_2+V_{3\beta}T_3+V_{4\beta}T_4+V_{0\beta}T_0=V_\beta^* T_1\\ V_{1z3}T_1+V_{2z3}T_2+V_{3z3}T_3+V_{4z3}T_4+V_{0z3}T_0=0\\ V_{1z4}T_1+V_{2z4}T_2+V_{3z4}T_3+V_{4z4}T_4+V_{0z4}T_0=0\\ T_1+T_2+T_3+T_4+T_0=T_s\end{cases} \tag{16}$$

V_1, V_2, V_3 and V_4 are four adjacent active vectors in each sector; and T_1, T_2, T_3 and T_4 are their corresponding time intervals. Also V_0 and T_0 are zero vector and its corresponding time interval respectively. For example, for the first sector $(0<\theta<60)$ V_1, V_2, V_3 and V_4

TABLE 2. Categorization of space vectors based on CMV value

Number of switching states	CMV Value
141	**0**
252	$\pm\frac{V_{dc}}{12}$
180	$\pm\frac{V_{dc}}{6}$
100	$\pm\frac{V_{dc}}{4}$
42	$\pm\frac{V_{dc}}{3}$
12	$\pm\frac{5V_{dc}}{12}$
2	$\pm\frac{V_{dc}}{2}$

corresponds to V_{494}, V_{650}, V_{702} and V_{234} respectively. Based on Equation (16), the time intervals can be calculated as follow:

$$\begin{bmatrix} T_1 \\ T_2 \\ T_3 \\ T_4 \\ T_0 \end{bmatrix} = \begin{bmatrix} V_{1\alpha} & V_{2\alpha} & V_{3\alpha} & V_{4\alpha} & V_{0\alpha} \\ V_{1\beta} & V_{2\beta} & V_{3\beta} & V_{4\beta} & V_{0\beta} \\ V_{1z3} & V_{2z3} & V_{3z3} & V_{4z3} & V_{0z3} \\ V_{1z4} & V_{2z4} & V_{3z4} & V_{4z4} & V_{0z4} \\ 1 & 1 & 1 & 1 & 1 \end{bmatrix}^{-1} \begin{bmatrix} V_\alpha^* T_s \\ V_\beta^* T_s \\ 0 \\ 0 \\ T_s \end{bmatrix} \tag{17}$$

As shown in Figure 2, all the selected space vectors in the z_3-z_4 plane are located in the second and fourth quarters which z_3 and z_4 components have same amplitude with opposite sign. So, the 3rd and 4th rows of 5×5 matrix in Equation (17) are symmetric and it cannot be reversed. Therefore, the time intervals cannot be calculated by considering zero avarage voltage in the z_3-z_4 plane during T_s. So, Equation (16) can be rewritten as Equation (18) and the time intervals is calculated by Equation (19).

$$\begin{cases} V_{1\alpha} T_1 + V_{2\alpha} T_2 + V_{0\alpha} T_0 = V_\alpha^* T_1 \\ V_{1\beta} T_1 + V_{2\beta} T_2 + V_{0\beta} T_0 = V_\beta^* T_1 \\ T_1 + T_2 + T_0 = T_s \end{cases} \tag{18}$$

$$\begin{bmatrix} T_1 \\ T_2 \\ T_0 \end{bmatrix} = \begin{bmatrix} V_{1\alpha} & V_{2\alpha} & 0 \\ V_{1\beta} & V_{2\beta} & 0 \\ 1 & 1 & 1 \end{bmatrix}^{-1} \begin{bmatrix} V_\alpha^* T_s \\ V_\beta^* T_s \\ T_s \end{bmatrix} \tag{19}$$

The selected space vectors can be applied according to state sequence shown in Figure 3 for the first sector ($0 < \theta < 60$). Although the adjacent active vectors in the α-β plane have opposite direction in the z_3-z_4 plane, during time interval T_S the closer space vector to the reference vector has bigger time interval and cosequently the average voltage on the z_3-z_4 plane is not zero. So, these nonzero voltages generate harmonic currents in the z_3-z_4 plane. These currents may be too much large if the machine leakage inductance is little.

The second group with 1 pu amplitude in the α-β plane and no z-component and CMV generation is shown in Figure 4. In other words, the only vectors with no z-component voltage and CMV between all 729 vectors belong to this group.

Figure 5 illustrates the state sequence of each phase for using second group space vectors, and shows zero value for CMV. Whereas the selected space vectors have no projection in the z_1-z_2 and z_3-z_4 planes, it needs to consider just volt-second balance in the α-β plane. Therefore, the time intervals T_1, T_2 and T_0 can be calculated by Equation (19).

4. 2. Asymmetrical SPIM Similar to symmetrical SPIM, high amplitude in the α-β plane and minimum amplitude in the z_1-z_2 and z_3-z_4 planes must be considered

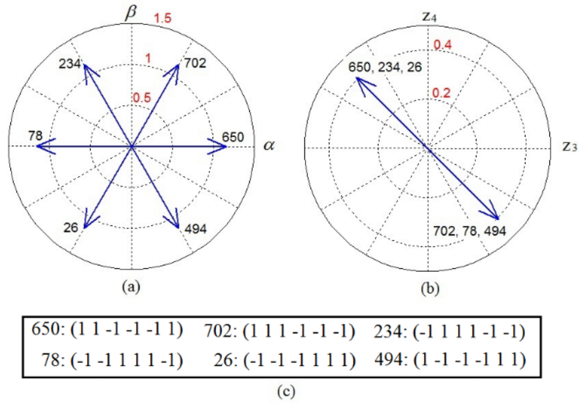

Figure 2. Selected space vectors in symmetrical SPIM with highest amplitude (1.15 pu) in the α-β plane: a) projection in the α-β plane, b) projection in the z_3-z_4 plane, c) corresponding switches state for each vector

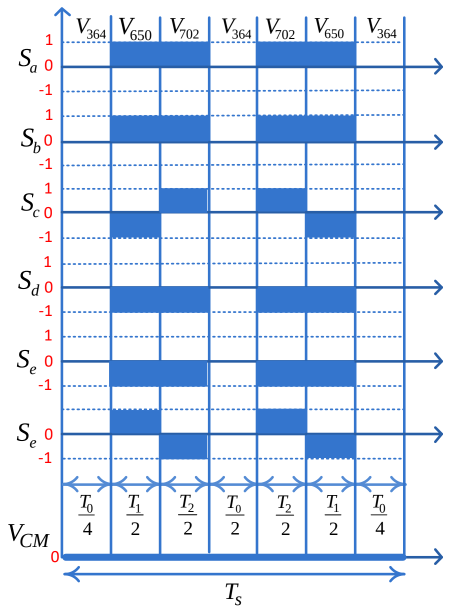

Figure.3 The state sequence of inverter for the first sector (0<θ<60) by applying space vectors with highest amplitude (1.15 pu) in the α-β plane for symmetrical SPIM

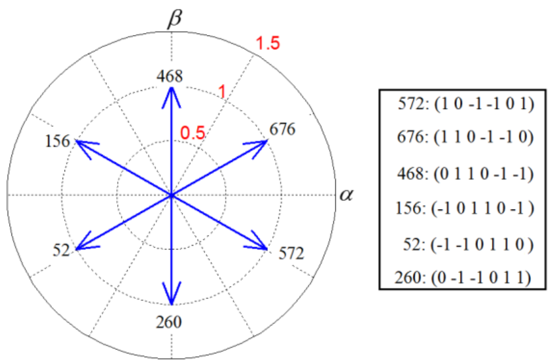

Figure 4. Selected space vectors in symmetrical SPIM with 1pu amplitude in the α-β plane

for space vector selection. The first vector group with highest amplitude in the α-β plane (1.11 pu) is depicted in Figure 6. The selected space vectors have 0.3 pu amplitude in the z_1-z_2 and 0 or 0.4 pu amplitude in the z_3-z_4 plane. The sum of switches state for the selected space vectors is 0 or ±2. So, based on Equation (15), produced CMV has 0 or $\pm\frac{V_{dc}}{6}$ amplitude.

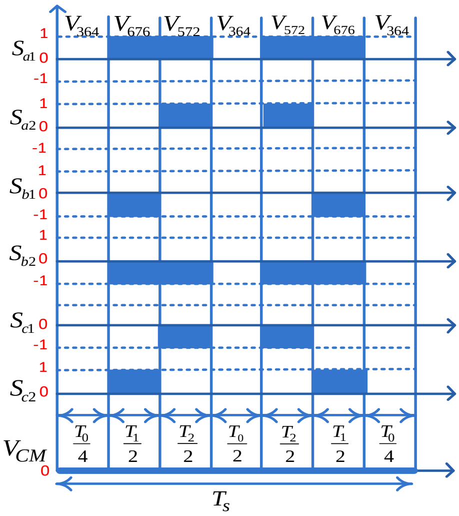

Figure 5. The state sequence of inverter for first sector (-30<θ<30) by applying space vectors with 1 pu amplitude in the α-β plane for symmetrical SPIM

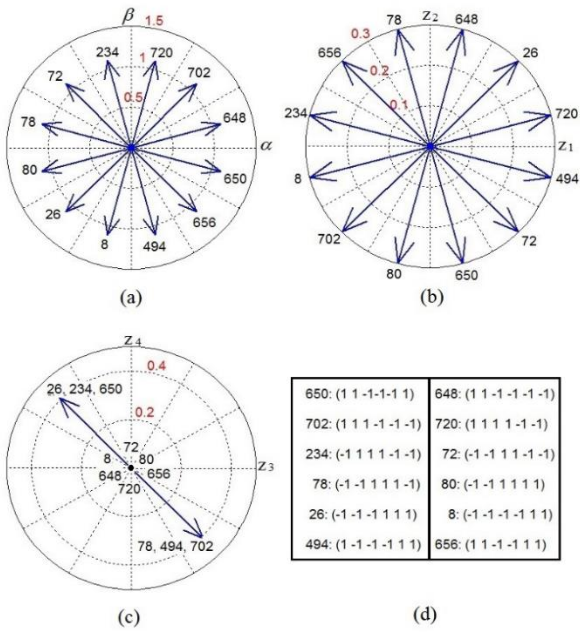

Figure 6. Selected space vectors in asymmetrical SPIM with highest amplitude (1.11pu) in the α-β plane: a) projection in the α-β plane, b) projection in the z_1-z_2 plane, c) projection in the z_3-z_4 plane, d) corresponding switches state for each vector

Similar to the first space vectors group in the symmetrical SPIM (Section 4.1), the selected space vectors are located in 2nd and 4th quarters in the z_3-z_4 plane and consequently the time interval equation cannot be solved. So, volt-second balance just can be considered in α-β and z_1-z_2 planes, and four adjacent vectors can be selected for each sector to calculate the time intervals. For example, space vectors number 656, 650, 648 and 702 can be used for the first sector ($-15<\theta<15$). Therefore, the time intervals can be calculated as follow:

$$\begin{bmatrix} T_1 \\ T_2 \\ T_3 \\ T_4 \\ T_0 \end{bmatrix} = \begin{bmatrix} V_{1\alpha} & V_{2\alpha} & V_{3\alpha} & V_{4\alpha} & V_{0\alpha} \\ V_{1\beta} & V_{2\beta} & V_{3\beta} & V_{4\beta} & V_{0\beta} \\ V_{1z1} & V_{2z1} & V_{3z1} & V_{4z1} & V_{0z1} \\ V_{1z2} & V_{2z2} & V_{3z2} & V_{4z2} & V_{0z2} \\ 1 & 1 & 1 & 1 & 1 \end{bmatrix}^{-1} \begin{bmatrix} V_\alpha^* T_s \\ V_\beta^* T_s \\ 0 \\ 0 \\ T_s \end{bmatrix} \tag{20}$$

The state sequence for the first sector is depicted in Figure 7. As can be seen, changing the switches state during each sampling period T_s is more than two previous PWM patterns shown for symmetrical SPIM, and leads to higher switching losses.

The second vector group with 1.07 pu amplitude in the α-β plane is depicted in Figure 8. The projection of the selected space vectors in the α-β, z_1-z_2 and z_3-z_4 planes have similar characteristics to the first group, and consequently the time intervals is calculated by Equation (20). But the selected space vectors have smaller amplitude in the z_1-z_2 and z_3-z_4 planes compared to the first group. The sum of switches state for the selected space vectors is ±1, and based on Equation (15), the

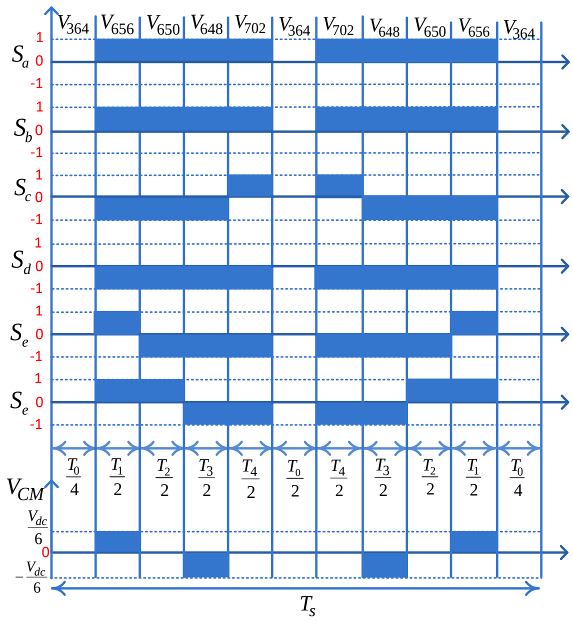

Figure 7. The state sequence of inverter for the first sector (-15<θ<15) by applying space vectors with 1.11 pu amplitude in the α-β plane for asymmetrical SPIM

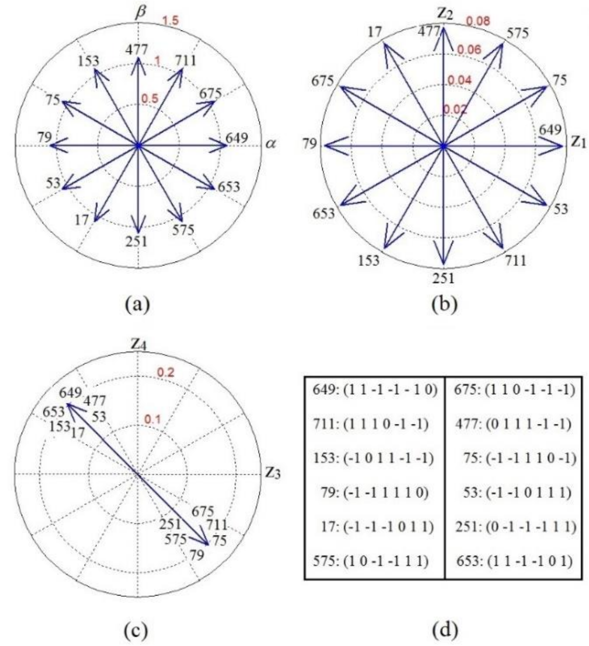

649: (1 1 -1 -1 - 1 0)	675: (1 1 0 -1 -1 -1)
711: (1 1 1 0 -1 -1)	477: (0 1 1 1 -1 -1)
153: (-1 0 1 1 -1 -1)	75: (-1 -1 1 1 0 -1)
79: (-1 -1 1 1 1 0)	53: (-1 -1 0 1 1 1)
17: (-1 -1 -1 0 1 1)	251: (0 -1 -1 -1 1 1)
575: (1 0 -1 -1 1 1)	653: (1 1 -1 -1 0 1)

Figure 8. Selected space vectors in asymmetrical SPIM with 1.07 pu amplitude in the α-β plane: a) projection in the α-β plane, b) projection in the z_1-z_2 plane, c) projection in the z_3-z_4 plane, d) corresponding switches state for each vector

produced CMV has $\pm\frac{V_{dc}}{12}$ amplitude. The state sequence of each phase for the first sector (0<θ<60) is depicted in Figure 9. It can be seen that the number of phases state changing is equal to the first group but the resulted CMV has lower peak to peak value.

The third space vector group is depicted in Figure 10 with 0.97 pu and 0.26 pu amplitudes in the α-β and z_1-z_2 plans respectively. The selected space vectors produce no CMV and have no projection in the z_3-z_4 plane. So, the time intervals can be calculated by Equation (20). The state sequence illustrated in Figure 11 shows lower phases state changing compared to two previous space vector groups.

5. SIMULATION RESULTS

The described SVPWM techniques are simulated by Matlab/Simulink software and shown in Figures 12-16. The system parameters are given in Table 3 and the PWM techniques are named in Table 4. The modulation index and frequency is set to 1 and 50 Hz respectively, and the mechanical load is assumed to have a constant torque (40 Nm). As depicted in simulation results, all the methods have similar α-β current component approximately. The α-β currents in all PWM methods are balanced (same amplitude and 90^0 phase difference) with a small distortion which leads to torque ripple producing. But the difference in the phase currents is due to z-components as a result of different properties of the selected space vectors for each method.

The result of applying the SVPWM-1 method on symmetrical SPIM is depicted in Figure 12. As explained in Section 4.1, no z_1-z_2 current and CMV is produced in this method. But, having nonzero average voltage in each sampling time interval (T_s) in the z_3-z_4 plane results in high z_3 and z_4 current components with frequency of $3f_s$.

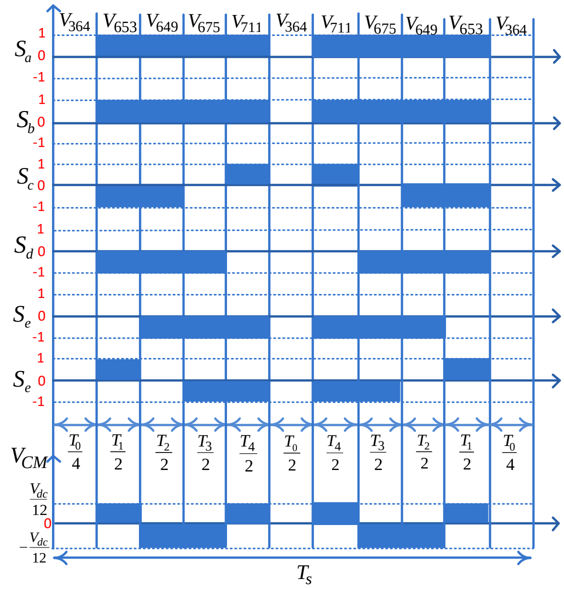

Figure 9. The state sequence of inverter for the first sector (0<θ<30) by applying space vectors with 1.07 pu amplitude in the α-β plane for asymmetrical SPIM

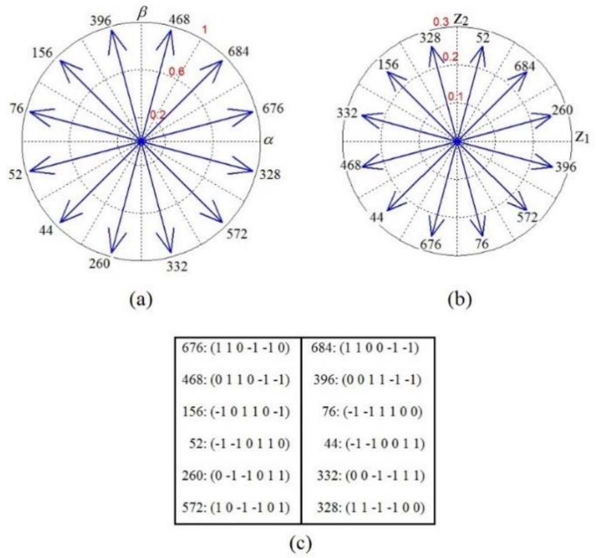

676: (1 1 0 -1 -1 0)	684: (1 1 0 0 -1 -1)
468: (0 1 1 0 -1 -1)	396: (0 0 1 1 -1 -1)
156: (-1 0 1 1 0 -1)	76: (-1 -1 1 1 0 0)
52: (-1 -1 0 1 1 0)	44: (-1 -1 0 0 1 1)
260: (0 -1 -1 0 1 1)	332: (0 0 -1 -1 1 1)
572: (1 0 -1 -1 0 1)	328: (1 1 -1 -1 0 0)

Figure 10. Selected space vectors in asymmetrical SPIM with 0.97 pu amplitude in the α-β plane: a) projection in the α-β plane, b) projection in the z_1-z_2 plane, c) corresponding switches state for each vector

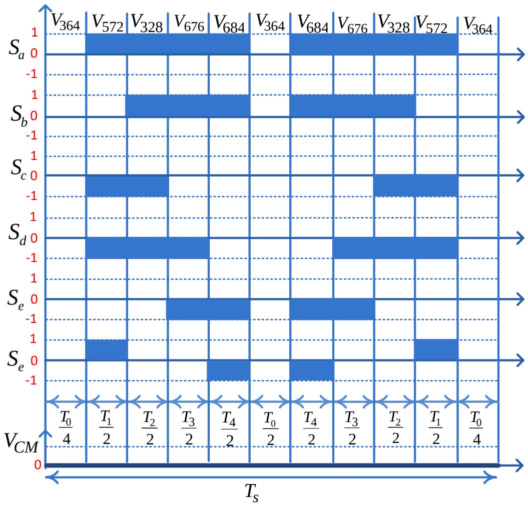

Figure 11. The state sequence of inverter for the first sector (-15<θ<15) by applying space vectors with 0.97 pu amplitude in the α-β plane for asymmetrical SPIM

TABLE 3. Parameters of the simulated motor [23]

Inverter DC voltage	600 V
Number of Pole pairs	4
Mutual inductance	51.3 mH
Stator resistance	2.34 Ω
Stator leakage inductance	6.7 mH
Rotor resistance	1.17 Ω
Rotor leakage inductance	6.7 mH
Inertia coefficient	0.03 kg.m^2

TABLE 4. Naming of several SVPWM technique based on SPIM configuration and space vectores amplitude in the α-β plane

SPIM configuration	Amplitude in the α-β plane	name
Symmetrical	1.15 pu	SVPWM-1
	1 pu	SVPWM-2
Asymmetrical	1.11 pu	SVPWM-3
	1.077 pu	SVPWM-4
	0.97 pu	SVPWM-5

So, the generated z_3 and z_4 current components appear as high 3rd harmonic in the stator currents and cause high current losses in the drive system. Hence, this PWM method is not applicable.

Figure 13 shows the result of applying the SVPWM-2 method on symmetrical SPIM. As can be seen, no z-component current and CMV are produced and the resulting phase currents are sinusoidal. Moreover, the electromagnetic torque has less ripple compared to the SVPWM-1 method.

The results of applying SVPWM-3 and SVPWM-4 on the asymmetrical SPIM are depicted in Figures 14 and 15, respectively, and both of them produce high z_3 and z_4 current components with frequency of $3f_s$ leading to presence of high 3rd harmonic in the stator phase currents. The CMV produced by SVPWM-3 and SVPWM-4 have $V_{dc}/6$ and $V_{dc}/12$ peak amplitudes respectively.

As illustrated in Figure 16, applying the SVPWM-5 with smaller space vectors amplitude in the α-β plane compared to two previous methods, produces no CMV and z_3-z_4 current components and the resulted z_1-z_2 current components are insignificant.

Based on simulation results, just SVPWM-2 and SVPWM-5 respectively for symmetrical and asymmetrical SPIM configurations are applicable. So, this two PWM methods are compared in the next simulation results as proposed the PWM techniques for both symmetrical and asymmetrical SPIM configurations.

Changing of one phase switches state during *Ts* in the first sector are shown in Figures 17 and 18 for SVPWM-2 and SVPWM-5 methods respectively. In SVPWM-2 two switches in each phase have no state changing, and the state of other switches is changed through two pulses. However, in the other sectors this is different and the constant state belongs to other switches. But, the switches in SVPWM-5 have more state changing which leads to higher switching losses.

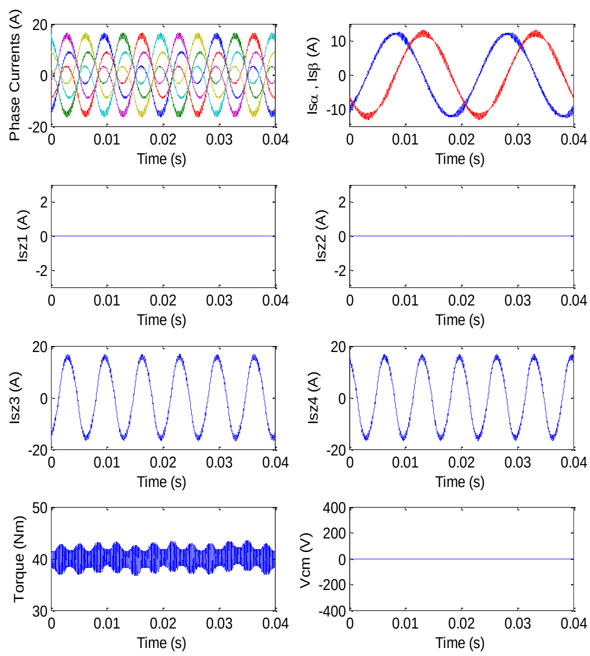

Figure 12. Simulation results of applying SVPWM-1 on the symmetrical SPIM

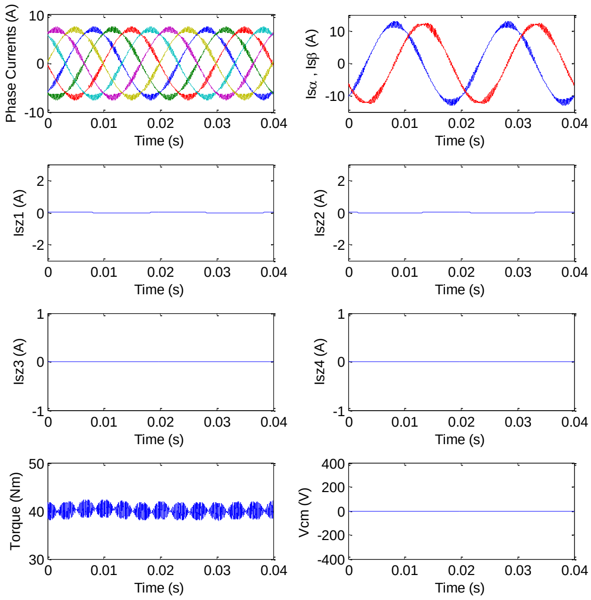

Figure 13. Simulation results of applying SVPWM-2 on the symmetrical SPIM

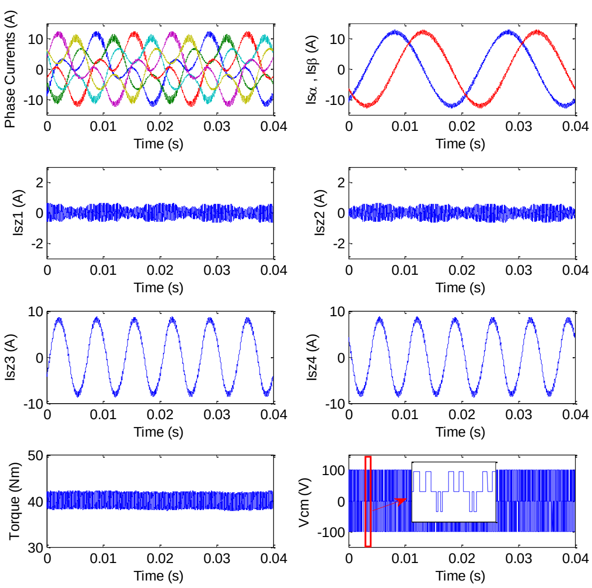

Figure 14. Simulation results of applying SVPWM-3 on the asymmetrical SPIM

Figure 19 shows the ratio between rms value of z-components to α-β voltages versus modulation index for SVPWM-2 and SVPWM-5 methods. The ratio is calculated by Equation (21) and describes the presence of undesired (z-components) voltages compared to the α-β components in the stator phase voltages.

$$\frac{V_z}{V_{\alpha\beta}} = \frac{\sqrt{V_{z1}^2 + V_{z2}^2 + V_{z3}^2 + V_{z4}^2}}{\sqrt{V_\alpha^2 + V_\beta^2}} \tag{21}$$

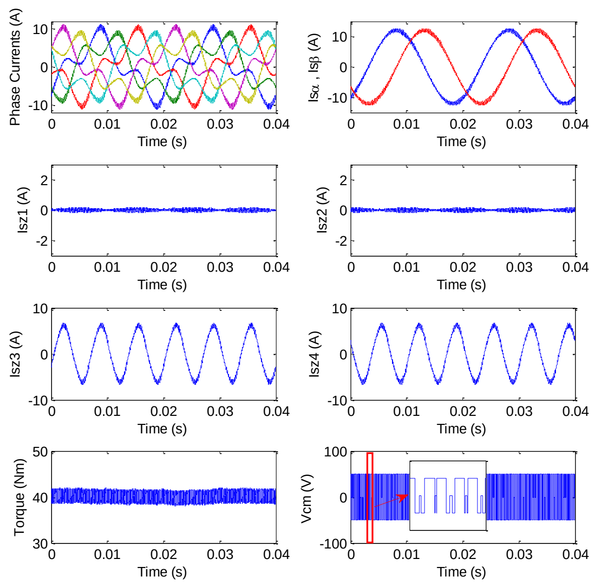

Figure 15. Simulation results of applying SVPWM-4 on the asymmetrical SPIM

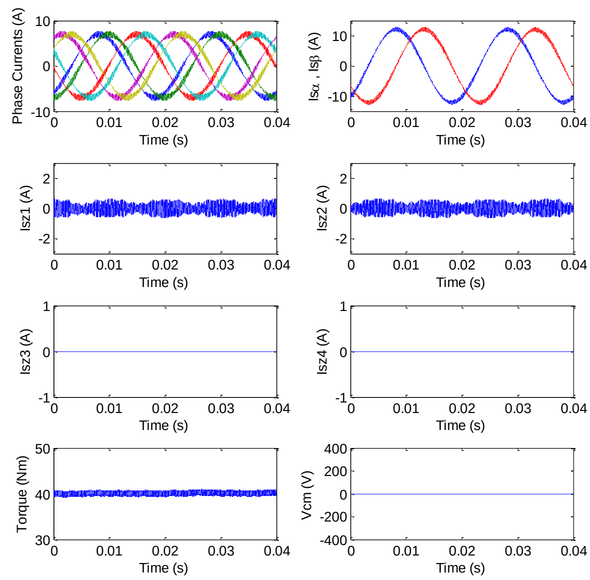

Figure 16. Simulation results of applying SVPWM-5 on the asymmetrical SPIM

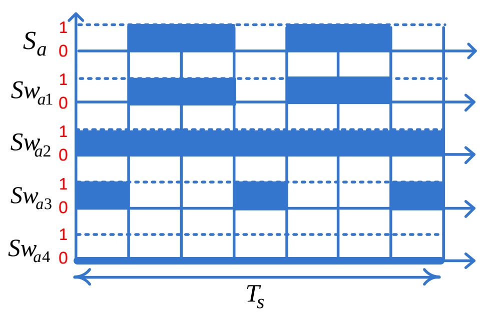

Figure 17. The switching sequence of "a" phase switches for symmetrical SPIM and selected space vectors with 1pu amplitude in the α-β plane

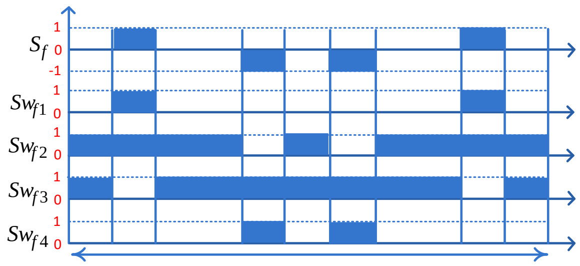

Figure 18. The switching sequence of "*f*" phase switches for asymmetrical SPIM and selected space vectors with 0.97pu amplitude in the *α*-*β* plane

The selected space vectors in SVPWM-2 have no z-component voltage and the resulted $V_z / V_{\alpha\beta}$ ratio is zero. On the other hand, the zero vector V_{364} (0 0 0 0 0 0) applied for SVPWM-5 has no *α*-*β* and z-components, and the time interval of applying active vectors in the *α*-*β* and z_1-z_2 planes are the same. So, the $V_z / V_{\alpha\beta}$ ratio for this PWM method is constant and equals to the ratio between space vectors amplitude in the z_1-z_2 plane to the *α*-*β* as shown in Equation (22).

$$\frac{V_z}{V_{\alpha\beta}} = \frac{|V_{z1-z2}|}{|V_{\alpha-\beta}|} = \frac{0.26}{0.97} = 0.268 \tag{22}$$

However, the SVPWM-5 produces a considerable z-component voltage compared to the SVPWM-2, but as shown in Figure 20, the phase voltage THD for both methods has a little difference in all modulation index values.

The phase currents FFT analysis in both of the methods for m=0.6 and f=30 Hz are compared in Figure 21, which shows a slight difference in current THD. Since in the SVPWM-2 method no z-component voltage is produced and has the same current distortion compared to SVPWM-5 method, it can be concluded that the former has more *α*-*β* current distortion than the latter. So, the resulted electromagnetic torque in SVPWM-2 method has more ripple than SVPWM-5 method, and it can be seen by comparing the torque waveforms in Figure 13 with Figure 16 in which the torque ripples for SVPWM-2 and SVPWM-5 methods are 9.12 and 3.7% respectively.

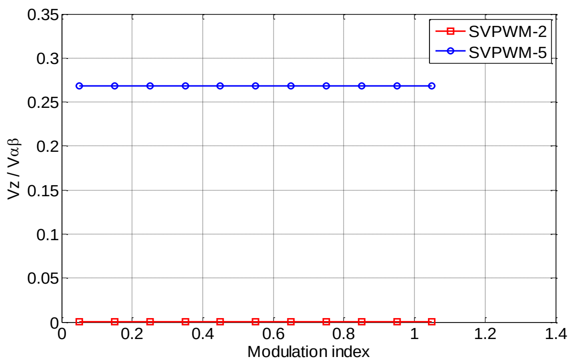

Figure 19. z-components to *α*-*β* voltages ratio versus modulation index for SVPWM-2 and SVPWM-5 methods

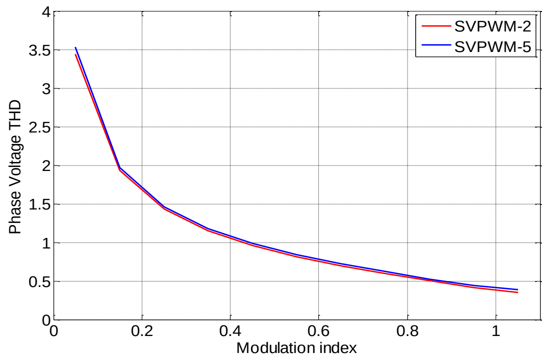

Figure 20. Phase voltages THD versus modulation index for SVPWM-2 and SVPWM-5 methods

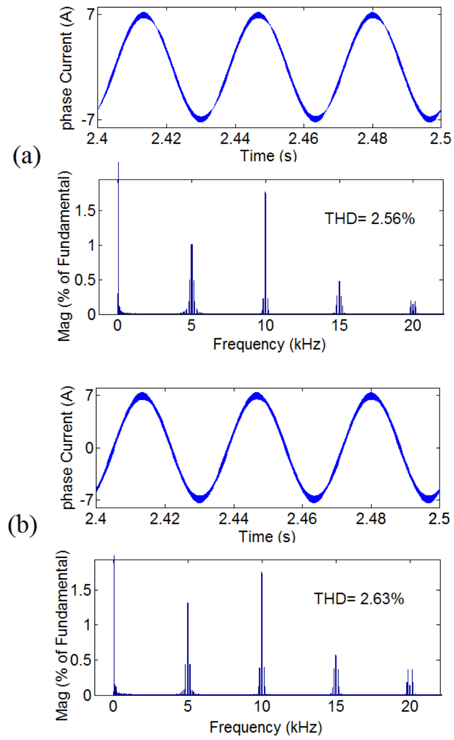

Figure 21. Phase current and FFT spectrum for m=0.6 and 30 Hz reference voltage: a) SVPWM-2 method, b) SVPWM-5 method

6. CONCLUSION

A comprehensive analysis of the SVPWM strategies for both symmetrical and asymmetrical six-phase induction motor drive with three-level inverter was given in this paper. The space vectors were selected and applied in each PWM method based on maximum α-β voltage, minimum z-component current, and CMV production. Based on theoretical analysis and simulation results, it is shown that just SVPWM-2 and SVPWM-5 methods with lower amplitude in the α-β plane for symmetrical and asymmetrical SPIM respectively are applicable. Both of the PWM methods produce no CMV but SVPWM-5 produces a slight z_1-z_2 current component while no z-component current is generated by SVPWM-2 method. The comparison of the number of switches state changing during the sampling time interval shows that SVPWM-2 has lower switching compared to SVPWM-5 strategy and leads to lower switching losses. On the other hand, both of the PWM methods have the same voltage and current THD approximately, and the generated electromagnetic torque has lower ripple in SVPWM-5 method. However, high frequency electromagnetic torque ripple can be damped by the machine mechanical system specially in larger machines. So, the symmetrical SPIM with SVPWM-2 strategy can be a better configuration for six-phase drive system. However, applying three-level inverter in a six-phase drive system imposes additional costs, but it leads to longer machine life time and a considerable modification in efficiency due to CMV and z-component currents elimination and lower switching losses.

7. REFERENCES

1. Nguyen, N.K., Meinguet, F., Semail, E. and Kestelyn, X., "Fault-tolerant operation of an open-end winding five-phase pmsm drive with short-circuit inverter fault", ***IEEE Transactions on Industrial Electronics***, Vol. 63, No. 1, (2015), 595-605.
2. Ericsen, T., "The ship power electronic revolution: Issues and answers", in 2008 55th IEEE Petroleum and Chemical Industry Technical Conference, IEEE., (2008), 1-11.
3. Levi, E., "Multiphase electric machines for variable-speed applications", ***IEEE Transactions on Industrial Electronics***, Vol. 55, No. 5, (2008), 1893-1909.
4. Abbas, M.A., Christen, R. and Jahns, T.M., "Six-phase voltage source inverter driven induction motor", ***IEEE Transactions on Industry Applications***, Vol., No. 5, (1984), 1251-1259.
5. Ariff, E.A.R.B.E. and Dordevic, O., "Space vector pwm technique for a two-level asymmetrical six-phase drive", ***The Journal of Engineering***, Vol. 2019, No. 17, (2019), 3878-3883.
6. Ariff, E.A.R.E., Dordevic, O. and Jones, M., "A space vector pwm technique for a three-level symmetrical six-phase drive", ***IEEE Transactions on Industrial Electronics***, Vol. 64, No. 11, (2017), 8396-8405.
7. Kianinezhad, R., Nahid, B., Betin, F. and Capolino, G.-A., "Multi-vector svm: A new approach to space vector modulation control for six-phase induction machines", in 31st Annual Conference of IEEE Industrial Electronics Society, 2005. IECON 2005., IEEE., (2005).
8. Xu, L. and Ye, L., "Analysis of a novel stator winding structure minimizing harmonic current and torque ripple for dual six-step converter-fed high power ac machines", ***IEEE Transactions on Industry Applications***, Vol. 31, No. 1, (1995), 84-90.
9. Zhao, Y. and Lipo, T.A., "Space vector pwm control of dual three-phase induction machine using vector space decomposition", ***IEEE Transactions on Industry Applications***, Vol. 31, No. 5, (1995), 1100-1109.
10. Karugaba, S., Muetze, A. and Ojo, O., "On the common-mode voltage in multilevel multiphase single-and double-ended diode-clamped voltage-source inverter systems", ***IEEE Transactions on Industry Applications***, Vol. 48, No. 6, (2012), 2079-2091.
11. Payami, S., Behera, R.K., Iqbal, A. and Al-Ammari, R., "Common-mode voltage and vibration mitigation of a five-phase three-level npc inverter-fed induction motor drive system", ***IEEE Journal of Emerging and Selected Topics in Power Electronics***, Vol. 3, No. 2, (2014), 349-361.
12. Zhang, R., Wu, X. and Wang, T., "Analysis of common mode emi for three-phase voltage source converters", in IEEE 34th Annual Conference on Power Electronics Specialist, 2003. PESC'03., IEEE. Vol. 4, (2003), 1510-1515.
13. Liu, Z., Zheng, Z., Sudhoff, S.D., Gu, C. and Li, Y., "Reduction of common-mode voltage in multiphase two-level inverters using spwm with phase-shifted carriers", ***IEEE Transactions on Power Electronics***, Vol. 31, No. 9, (2015), 6631-6645.
14. Tan, C., Xiao, D., Fletcher, J.E. and Rahman, M.F., "Carrier-based pwm methods with common-mode voltage reduction for five-phase coupled inductor inverter", ***IEEE Transactions on Industrial Electronics***, Vol. 63, No. 1, (2015), 526-537.
15. Tan, C., Xiao, D., Fletcher, J.E. and Rahman, M.F., "Analytical and experimental comparison of carrier-based pwm methods for the five-phase coupled-inductor inverter", ***IEEE Transactions on Industrial Electronics***, Vol. 63, No. 12, (2016), 7328-7338.
16. Chen, K.-Y. and Hsieh, M.-S., "Generalized minimum common-mode voltage pwm for two-level multiphase vsis considering reference order", ***IEEE Transactions on Power Electronics***, Vol. 32, No. 8, (2016), 6493-6509.
17. López, Ó., Alvarez, J., Malvar, J., Yepes, A.G., Vidal, A., Baneira, F., Pérez-Estévez, D., Freijedo, F.D. and Doval-Gandoy, J., "Space-vector pwm with common-mode voltage elimination for multiphase drives", ***IEEE Transactions on Power Electronics***, Vol. 31, No. 12, (2016), 8151-8161.
18. Durán, M.J., Prieto, J., Barrero, F., Riveros, J.A. and Guzman, H., "Space-vector pwm with reduced common-mode voltage for five-phase induction motor drives", ***IEEE Transactions on Industrial Electronics***, Vol. 60, No. 10, (2012), 4159-4168.
19. Duran, M.J., Prieto, J. and Barrero, F., "Space vector pwm with reduced common-mode voltage for five-phase induction motor drives operating in overmodulation zone", ***IEEE Transactions on Power Electronics***, Vol. 28, No. 8, (2012), 4030-4040.
20. Dabour, S.M., Abdel-Khalik, A.S., Ahmed, S., Massoud, A.M. and Allam, S., "Common-mode voltage reduction for space vector modulated three-to five-phase indirect matrix converter", ***International Journal of Electrical Power & Energy Systems***, Vol. 95, No., (2018), 266-274.
21. Zandzadeh, M.J., Kianinezhad, R. and Saniei, M., "Comparative analysis of space vector pwm for six-phase induction motor configurations based on common-mode voltage and current losses", ***Iranian Journal of Science and Technology, Transactions of Electrical Engineering***, Vol. 43, No. 4, (2019), 897-908.
22. Hadiouche, D., "Modelling of a double-star induction motor with an arbitrary shift angle between its three phase windings", ***EPE-PEMC'2000, Kosice, Slovak Republic, 5-7 September***, Vol. 5, No., (2000), 125-130.
23. Kianinezhad, R., Nahid-Mobarakeh, B., Baghli, L., Betin, F. and Capolino, G.-A., "Torque ripples suppression for six-phase induction motors under open phase faults", in IECON 2006-32nd Annual Conference on IEEE Industrial Electronics, IEEE., (2006), 1363-1368.

.

Persian Abstract

چکیده

افزایش روز افزون در به کارگیری سیستمهای درایو چند فاز باعث توسعه ساختار اینورترها و روشهای کنترلی به کار گرفته شده برای آنها شده است. تولید ولتاژ حالت مشترک توسط اینورتر، خرابی بیرینگها را در درایوهای چند فاز به دنبال دارد. از طرف دیگر حضور جریاتهای مولفه **z** در ماشین القایی شش فاز باعث افزایش تلفات جریانی می‌شود که باید در در روش PWM مورد استفاده در نظر گرفته شود. در این مقاله نشان داده شده است که حضور جریانهای مولفه **z** و ولتاژ حالت مشترک دو عامل محدود کننده مهم در انتخاب بردارهای فضایی می‌باشند. بردارهای فضایی ولتاژ برای هر دو ساختار متقارن و نامتقارن ماشین القایی تغذیه شده با اینورتر سه سطحی در زیرفضاهای قائم نمایش داده شده و بر اساس مولفه‌های ولتاژی نامطلوب و ولتاژ حالت مشترک توصیف شده‌اند. سپس روشهای مدولاسیون SVPWM متقاوتی بر اساس تولید ولتاژ حالت مشترک و جریانهای مولفه **z** بررسی شده است. نهایتا بر اساس نتایج شیه سازی‌های صورت گرفته، یک روش SVPWM بهبود یافته با حداقل اغتشاش جریان، مولفه‌های جریانی نامطلوب و ولتاژ حالت مشترک و با ریپل گشتاور قابل قبول ارائه شده است.